Urban Mobility Swarms: towards a decentralized autonomous bicycle-sharing system

N. Coretti-Sanchez[1], J. Múgica[1], Q. Bowers[1], A. Grignard[1,3], E. Castelló Ferrer[1,2,4], L. Alonso[1], K. Larson[1]

[1]City Science, MIT Media Lab, Cambridge, USA
[2]Connection Science, MIT, Cambridge, USA
[3]Univ Lyon, LIRIS, UMR5205, France
[4]School of Science & Technology, IE University, Spain

***Abstract*— Urban mobility can often be categorized as a complex system—e.g., a nonlinear system composed of many interacting components with interdependent relationships. The growing trend towards shared, lightweight, and autonomous vehicles requires planning solutions that are less centralized and can manage the increasing complexities of new mobility. This research investigates planning strategies for shared micro-mobility systems, focusing on shared autonomous bicycles. Vehicle rebalancing within such systems poses a critical technical challenge and has substantial environmental and economic implications. To tackle this challenge, we propose a fully decentralized approach that allows autonomous bicycles to rebalance in a self-organizing manner via stigmergy, a bio-inspired mechanism for indirect communication. While the bicycles autonomously navigate their urban environment, they locally update RFID tags at intersections, leaving virtual pheromone trails that collectively guide each other toward high-demand areas. The efficacy of our approach is assessed through a realistic agent-based model of Cambridge, MA (USA). Results highlight the capacity of autonomous bicycles to rebalance in a self-organized manner, using strictly decentralized local communication, while significantly reducing the average user wait time compared to no rebalancing and random rebalancing. These findings emphasize the feasibility and potential of decentralized planning strategies in handling complexity within new mobility systems.**

I. Introduction

Modern urban transportation networks are composed of many interacting components that often give rise to a nonlinear behavior with many feedback loops [1]. Current research points towards electrification, sharing, autonomy, and lightweight design as key characteristics of future mobility platforms, leading to new modes such as shared autonomous micro-mobility services, including bicycles, tricycles, and scooters [2]–[7]. It is expected that these novel micro-mobility services will further increase the complexity of urban mobility systems and will require planning solutions that are flexible, adaptable, and robust [8]–[10]. Many existing methods optimize centralized, analytical planning solutions, which might not be transferable to highly complex transportation systems with large numbers of vehicles and a demanding real-time component [11]–[15]. Therefore, new solutions are needed.

Fully decentralized vehicle rebalancing poses a great operational challenge and has rarely been studied in shared micro-mobility services [16]–[18]. The rebalancing problem results from unbalanced user travel patterns that cause vehicles to accumulate in some areas while others get depleted [18], [19]. In current deployments, rebalancing is usually accomplished by human operators manually redistributing vehicles throughout the city in vans or trucks, according to centralized analysis and planning, with a very high environmental and economic impact [20], [21].

Within the field of shared micro-mobility, studies have addressed different strategies to tackle the rebalancing problem. In the case of bicycle sharing systems, previous studies have used static as well as dynamic methods for manual rebalancing in station-based [22]–[26] and dockless systems [27]–[30]. In static manual rebalancing strategies, vehicles are transported at night, during low-usage periods, while in dynamic manual rebalancing, vehicles are redistributed during the day while users utilize the vehicles. Some studies have also proposed hybrid manual rebalancing strategies that combine operator rebalancing with incentive-based user rebalancing. In these hybrid strategies, users receive monetary rewards for making trips that balance the system [31]–[33].

Looking into the future, however, self-driving vehicles represent a promising approach to tackling the rebalancing problem because vehicles could autonomously redistribute themselves to the locations where they are most needed. Several recent studies have proposed a diverse set of autonomous vehicle rebalancing methods for fleets of self-driving cars and taxis [34]–[40]. Nevertheless, very few studies have addressed autonomous rebalancing in micro-mobility systems (e.g., shared bicycles, tricycles, or scooters) [5], [7].

A. From centralized to decentralized systems

A common characteristic of existing rebalancing methods is that they rely on centralized planning. However, centralized urban transportation systems are often restricted in terms of scalability, suffer from bottlenecks and single points of failure, and pose greater risks in terms of potential data breaches [12], [15], [40], [41]. On the one hand, the introduction of autonomous self-driving vehicles can increase the complexity of urban mobility systems by making the fleets of vehicles more challenging to coordinate [9], [10]. On the other hand, it brings new opportunities regarding vehicle interactions and how these interactions impact system-level behavior. For instance, autonomy will provide vehicles with

the ability to communicate with other vehicles, citizens, and the urban infrastructure, as well as the agency to make decisions based on this communication [42], all of which can lead to new types of collective behavior [43].

Mature research fields such as swarm robotics have been proposing decentralized solutions for the past 30 years: autonomous robots can use simple behaviors and decentralized communication to self-organize group-level behaviors (e.g., to allocate tasks, aggregate, or transport objects cooperatively [44]–[48]). These self-organized systems have been shown to be scalable, robust, and adaptive to variations in the environment. These characteristics are critical for future urban mobility systems since they will be required to show robust and adaptive responses to complex and unforeseen scenarios such as unprecedented demand patterns, vehicle errors, or server failures [8], [12]. In this regard, there has been some initial research on the application of swarm intelligence mechanisms to urban mobility scenarios, such as bio-inspired *stigmergy* (i.e., indirect communication between agents using modifications to the environment, such as by leaving trails of pheromones). For instance, [49] proposed a stigmergy-based network for tourists that generates pheromone paths leading to places with high attractiveness, and [50] presented a stigmergy-based model to infer urban areas of high activity from positioning data. Regarding the routing of autonomous vehicles, [51] presents a stigmergy-based system for autonomous shared tricycles to collect urban trash.

B. Bio-inspired decentralized rebalancing for autonomous shared bicycles

Inspired by the field of swarm robotics, this article proposes a bio-inspired decentralized method for vehicle rebalancing in fleets of autonomous micro-mobility. In the proposed system, shared autonomous bicycles rebalance themselves in a self-organized and demand-responsive way. The proposed rebalancing method is based on stigmergy so that bicycles can coordinate without a centralized communication system [52], [53]. In other words, as bicycles autonomously identify user demand, they leave virtual pheromone trails via RFID tags located at road intersections to collectively guide each other towards high-demand areas. The results of this study demonstrate that the proposed system can significantly reduce wait times for users, compared to random autonomous rebalancing or no rebalancing, consequently improving user experience. The rest of the paper is structured as follows. Section II describes the agent-based model of an urban environment built for this study. The experimental setup and its simulation process are outlined in Section III. Section IV presents the study's results, followed by a discussion in Section V and conclusions in Section VI.

II. Urban Mobility Swarms: A Multi-Layer Agent-Based Model

The performance of the proposed system has been evaluated through a multi-layer agent-based simulation. Agent-based models have gained significant popularity as a means of analyzing the meso- and macroscopic dynamics in mobility systems due to their capability to analyze behaviors arising from the interactions among diverse entities such as vehicle fleets, users, and infrastructure [54].

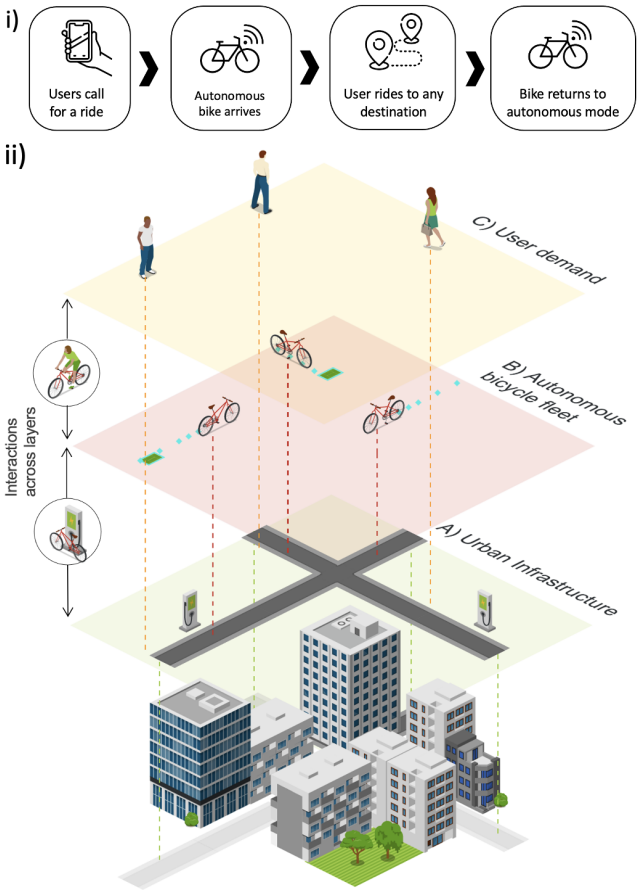

Fig. 1. Model behaviors, layers, and interactions. (i) Use of shared autonomous bicycles as a mobility-on-demand system. First, users call for bicycles through a mobile app. Second, the bicycles drive to pick up the user. Third, the users ride the bicycles to their destinations. Finally, the bicycles return to autonomous mode. (ii) Multi-layer architecture of the model: (A) Urban infrastructure (buildings, roads, charging stations), (B) Autonomous bicycle fleet, and (C) User demand.

The model represents the behavior of shared autonomous bicycles as a mobility-on-demand system (Fig. 1 i). First, users call for a ride through a mobile app. Second, the bicycle drives autonomously to the user's location. Third, the user rides the bicycles to their desired destination. Finally, once the user disembarks at the destination, the bicycle returns to autonomous mode to pick up the following user, drive towards higher-demand areas, or go to a charging station. Three essential layers are needed to model this behavior in a multi-bicycle system, which are detailed in the following subsections: A) the urban infrastructure, B) the fleet of shared autonomous micro-mobility bicycles, and C) the user demand. This multi-layer representation shows the different behaviors and interactions occurring across our system, such as bicycles interacting with urban infrastructure, users asking for a bicycle ride, or bicycles going to a charging station (Fig. 1 ii).

A. Urban infrastructure

The city is instantiated through geospatial data, which contains the road graph and buildings' shapefile data. These two datasets are used to recreate the urban infrastructure layer (Fig. 1 ii A). In our model, bicycles use the road network to travel around the city. Similarly, users start and end their trips in buildings and use the road network during these trips, simulating human behavior patterns such as the commute to work, shopping for groceries, or leisure trips, among others. Complementarily, the model contains urban infrastructure related to the operation of the autonomous micro-mobility system, specifically, charging stations (Fig. 1 ii A). For this study, charging stations are considered battery swapping stations to minimize the impact of station charging capacity and bicycle charging time on the global system performance.

B. Autonomous bicycle fleet

The next layer of our proposed model is the one containing the shared autonomous bicycle fleet (Fig. 1 ii B). In this section, first, we will describe the behavior of single bicycle agents. Then, we will describe the way bicycles communicate indirectly using stigmergy.

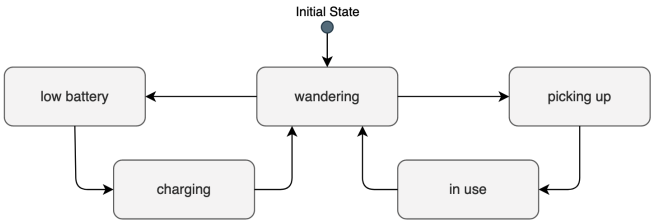

Fig. 2. Diagram depicting the bicycles' behavior as a finite-state machine (FSM). Bicycles initially wander around the city. They pick up users autonomously, and then users ride them to their destination. During this process, the bicycles use stigmergy as an indirect communication method. Once a bicycle drops off a user, it goes back to wandering. While wandering, if a bicycle's battery drops too low, it will go to a charging station.

1) Bicycle behavior: The diagram in Fig. 2 depicts the behavior of the bicycles, which is defined as a finite-state machine (FSM). All bicycles are initially in the *wandering* state. In this state, each bicycle will wander around the target urban area guided by the information previously left by all bicycles collectively. The bicycles read the information of the RFID tags located at the road intersections (Fig. 1 ii B) and follow the road with the highest demand (more details in Sec. II-B.2). Bicycles transition from the *wandering* state to the *picking up* state when they get a rider call. In the *picking up* state, bicycles will navigate to the rider's pick up point. They transition to the *in use* state (which includes transiting out of self-driving mode into manual mode) once they have reached their rider. While a bicycle is in the *in use* state, a user manually drives it to a destination. A bicycle transitions back to the *wandering* state once its rider completes the trip and disembarks. When in the *wandering* state, bicycles may also transition to the *low battery* state if their battery drops below a set threshold (in this case, when they reach 25% of battery capacity). The FSM is designed

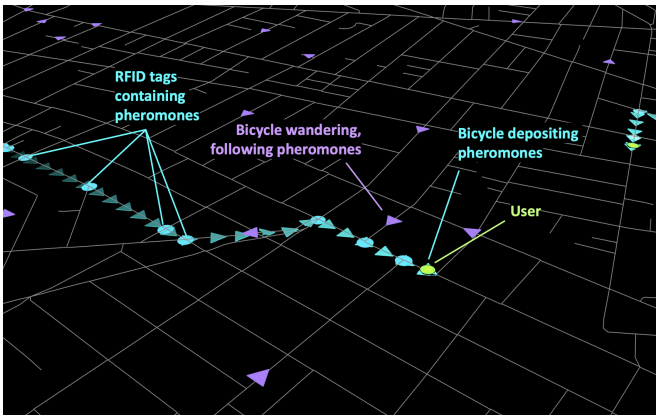

Fig. 3. Real-time snapshot of the simulation model showing the stigmergic behavior in the bicycle fleet. User demand (green dot), RFID tags (blue dots; darker blue indicates higher pheromone level), bicycles depositing pheromones while picking up a user or in use (blue triangles), wandering bicycles guided by pheromones (pink triangles). A video describing the key takeaways of this research is available here: https://bit.ly/3o5wYEe

so that riders' trips will not be interrupted by bicycles redirecting toward charging stations. In the *low battery* state, a bicycle immediately seeks out the nearest charging station and transitions to the *charging* state when it arrives at the station. In the *charging* state, a bicycle idles at the charging station. A bicycle transitions back to the *wandering* state once its battery has been swapped.

2) Stigmergic behavior: While wandering, the autonomous bicycle fleet communicates in a decentralized and indirect way using a stigmergy algorithm (Fig. 3). Stigmergy is a decentralized process that allows agents to communicate indirectly using environmental modifications, cooperating without any centralized coordination [52]. In nature, social animals (e.g., bees, ants) use stigmergy by, for instance, leaving trails of chemical pheromones in the environment. In this paper, stigmergy is achieved by locally storing and updating *virtual pheromones* in RFID tags located at road intersections analogously to [51]. Vehicles can read and write information from the RFID tags, such as unique IDs, timestamps of the last update, virtual pheromone levels for each intersecting road direction, and location of the closest charging station. Each time a bicycle passes through an intersection, there is a two-way interaction. Vehicles read the RFID tag and update the stored pheromone information according to evaporation, diffusion, and marking mechanisms, inspired by natural pheromones:

Evaporation: When a bicycle reaches a tag, it reads the timestamp and pheromone values of the last write operation. As a first step, it decreases all pheromone values according to a predefined evaporation rate and time elapsed from the last update, as follows:

$$\boldsymbol{P}_{u,t} = \boldsymbol{P}_{t'} - E_r * (t - t'), \tag{1}$$

where $\boldsymbol{P}_{u,t}$ is an updated pheromone at the current time t, t' is the timestamp of the last write operation, $\boldsymbol{P}'_t$ is a pheromone level in t', and E_r is the evaporation rate.

Diffusion: After the evaporation process, a diffusion process is used. The goal of the diffusion process is to dilute

each intersection's pheromone levels among neighboring intersections, increasing the probability of bicycles finding the highest pheromone levels. The bicycle updates the tag's pheromone values based on the information it read at the last intersection, such that

$$\boldsymbol{P}_{d,t} = \boldsymbol{P}_{u,t} + D_r * P_{read,max}, \tag{2}$$

where $\boldsymbol{P}_{d,t}$ is a pheromone after the diffusion update, D_r is the diffusion rate, and $P_{d,max}$ represents the maximum pheromone value read at the previous intersection.

Marking: Lastly, if the bicycle is doing a pick-up or in use, it will mark the RFID tags by increasing a pheromone value to help guide bicycles toward user demand, as follows:

$$P_t = P_{d,t} + PM, \tag{3}$$

where PM is the pheromone level that a single bicycle can leave when marking its trail, and P_t is the new updated value that will be stored at the RFID tag, alongside the timestamp of the operation. Only the pheromone value associated with the direction that the bicycle is coming from is updated in this step. For pheromone values associated with other directions, $P_t = P_{d,t}$.

It is important to note that when bicycles wander, they choose their routes according to the pheromone levels read from the RFID tags (Fig. 3). When a bicycle arrives at an intersection, it will continue along the street with the highest pheromone level. However, the bicycles might randomly choose a direction with a probability inverse to a predefined exploitation rate (X_r). This process is called exploration and is intended to prevent agents from getting stuck at local optima, e.g., causing a bicycle to non-optimally confine itself to a specific area (see Sec. V).

C. User demand

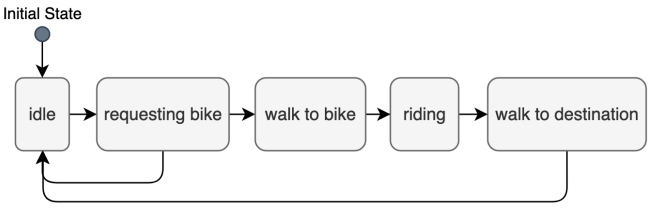

Fig. 4. Diagram depicting user behavior as an FSM. A user is initially in idle state, then requests a ride at a departure time, walks to meet the bicycle at an intersection, rides to the intersection closest to the destination, and walks from the intersection to the final destination.

The users of our system (Fig. 1 ii C) are also modeled through a FSM, as depicted in Fig. 4. In this FSM, users initially start in *idle* state. In *idle* state, users have no destination (i.e., this happens during the time a user is at home or at work). Idle users will transition to *requesting bike* state when they have a departure time. In the *requesting bike* state, the user is waiting for an available bicycle. In the *walk to bike* state, the user walks to its closest road intersection and waits there for the bicycle to arrive. From the *walk to bike* state, users will transition to the *riding* state when a bicycle arrives to pick the user up. In the *riding* state, the user manually drives the bicycle to an intersection near the destination. Users transition to the *walk to destination* state after having dropped the bicycle at an intersection near the destination. In the *walk to destination* state, users walk to the destination. Finally, users transition back to *idle* once they have reached their destination.

III. Experimental setup

A. Modeling software

The agent-based model described in Sec. II has been implemented in the GAMA platform [55], [56]; an open-source simulation tool that allows the development of multi-level agent-based models. GAMA has been used to model a variety of complex socio-environmental systems such as pandemic mitigation policies [57], urban decision-making processes [58], and urban mobility [59]. The code developed for this study is available on GitHub[1].

B. Selected site

Cambridge, MA, USA (Fig. 5 i) has been used as the urban infrastructure layer (Sec. II-A) due to the availability of shared bicycle usage data [60]. The geospatial data for this area (roads and buildings) have been obtained through OpenStreetMap [61].

Fig. 5. (i) Heatmap depicting the demand density (highest density areas are shown in violet) and the boundary of the area considered for this study (Cambridge, MA, USA). (ii) MIT Autonomous Bicycle [2], [6], [62], the target vehicle used in this paper and simulated in Sec. III. (iii) Top: Manual driving mode, with the rear wheels folded to act as a single wheel. Bottom: Self-driving mode, with the rear wheels unfolded for stability.

[1]GitHub: https://github.com/CityScope/VehicleClustering

TABLE I

SETS OF VALUES FOR EACH PARAMETER IN THE SIMULATION.

Parameter	Values	Unit	Description
N_b	[150, 250, 350]	[-]	Number of vehicles
W_s	[1, 3, 5]	[km/h]	Wandering speed
E_r	[0.05, 0.1, 0.15]	[0-1]	Evaporation rate
X_r	[0.6, 0.65, 0.7, 0.75, 0.8]	[0-1]	Exploitation rate

C. Demand modeling

User demand in the simulation is based on public usage data from the Bluebikes bicycles-sharing system [60] from October 12, 2019, for Cambridge, MA (Fig. 5 i), which contains a total of 1458 trips. The data was preprocessed by applying a randomized distribution function that scatters the origins and destinations of the trips in buildings within 300 m around Bluebikes docking stations, following the process detailed in [6]. This user-generation process yields realistic spatiotemporal usage patterns and avoids obstacles like rivers or highways. The average walking speed of users was considered 5 km/h [63], and their average riding speed was considered 10.2 km/h [64].

D. Vehicle modeling

The autonomous micro-mobility bicycle considered for this study is the MIT Autonomous Bicycle[2] (see Fig. 5 ii-iii), a vehicle developed at the MIT Media Lab City Science group that is designed to work as a shared and autonomous mobility-on-demand system [2], [6], [62]. In addition to the components needed for autonomous driving, this vehicle contains a mechanical system that allows the bicycle to transform into a tricycle during autonomous driving for lateral stability. When a user manually driving it, the system is in bicycle mode (see Fig. 5 iii, top). In this configuration, the two rear wheels act as a single wheel, and the riding experience remains unchanged from riding a regular bicycle. In contrast, when the bicycle is driving autonomously, the bicycle is in tricycle mode (see Fig. 5 iii, bottom). In this configuration, the wheels separate and provide the necessary lateral stability for self-driving.

The average speed in self-driving mode was set to 8 km/h, based on the specifications for the MIT Autonomous Bicycle project [6]. The battery autonomy was considered 30 km [4]. The location of the stations was determined by a k-means algorithm that generates locations for the charging stations based on intersection density. The model includes ten charging stations, with a capacity of 16 bicycles each. The capacity of each station is based on the average number and size of Bluebikes stations in the area under study [60]. The number of stations are based on vehicle and infrastructure needs in [6], [65]. The battery-swapping process has been considered to take 1.85 min; an average of the values reported in [66] for real stations of different brands.

The value of PM has been set to 0.01, while the value of D_r has been set to $0.5 * X_r$, based on [50]. Lastly, the number of bicycles (N_b), wandering speed (W_s), pheromone evaporation rate (E_r), and exploitation rate (X_r) are the most relevant variables to this study. Consequently, these variables have been treated as simulation parameters (Tab. I).

[2]MIT Autonomous Bicycle: https://bit.ly/3bTXTg3

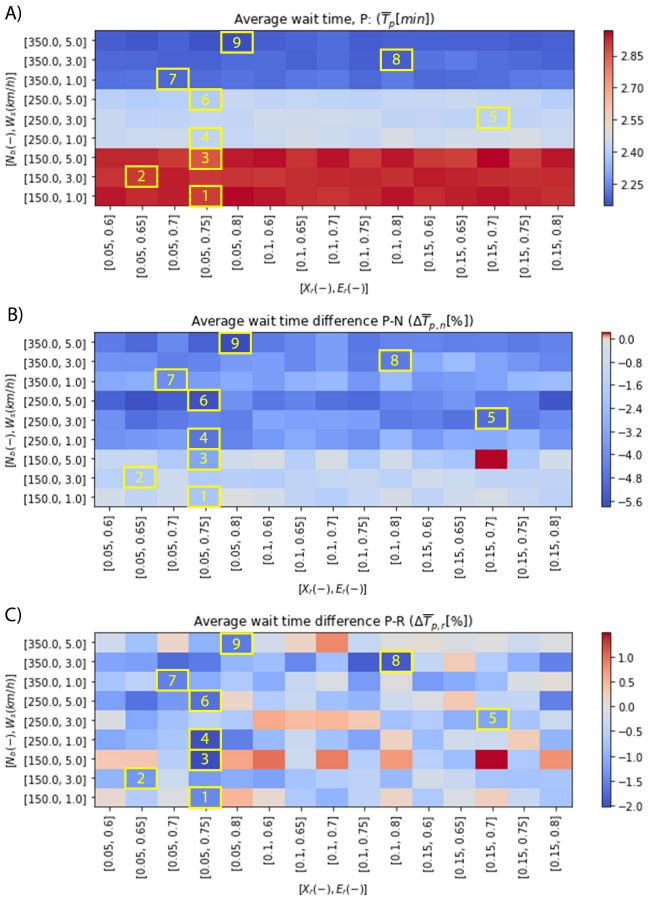

Fig. 6. Results for the different configuration parameters: (A) $\overline{T}$ (i.e., average user waiting time measured in minutes) in the pheromone-based rebalancing scenario, P, (B) Percentage difference in $\overline{T}$ of P over the nominal scenario, N, (C) Percentage difference in $\overline{T}$ of P over the random rebalancing scenario, R. Yellow boxes highlight the scenario with lowest $\overline{T}$ for each row (numbered according to Table II).

IV. RESULTS

In order to analyze the performance of the proposed approach, the metric chosen was the average time a user has to wait for a bicycle ($\overline{T}$), measured in minutes. To analyze the proposed approach, we consider three scenarios. First, the nominal scenario, N, was used as the baseline for this study, in which bicycles are not rebalanced. Second is the random rebalancing scenario, R, in which bicycles wander and choose their directions randomly at each road intersection. Third, in the pheromone-based rebalancing scenario, P, bicycles use our proposed stigmergy-based self-organized rebalancing system.

The results obtained for the different sets of N_b, W_s, E_r and X_r (Tab. I) can be found in Fig. 6. Results are an average of 15 independent runs for each parameter set, to account for stochasticity. This was found to be the number of runs needed to have reproducible results, and was determined by analyzing the convergence of $\overline{T}$, in 100 repetitions with identical parameters. Fig. 6 A shows $\overline{T}$ in P while Fig. 6 B

TABLE II

SIMULATION RESULTS INDICATING SYSTEM PERFORMANCE WITH OPTIMAL E_r AND X_r FOR EACH COMBINATION OF N_b AND W_s. SCENARIOS ARE HIGHLIGHTED AND NUMBERED IN FIG. 6.

Fig.7	Parameters				Results			
id	N_b	W_s[km/h]	E_r	X_r	$\overline{T}_p$[min]	$\Delta\overline{T}_{p,n}$[%]	$\Delta\overline{T}_{p,r}$[%]	D_p/D_n
1	150	1	0.05	0.75	2.90	-2.04	-1.46	1.97
2		3	0.05	0.65	2.91	-1.76	-1.31	4.13
3		5	0.05	0.75	2.86	-3.25	-2.03	6.29
4	250	1	0.05	0.75	2.42	-4.73	-1.99	2.66
5		3	0.15	0.7	2.41	-4.93	-1.16	6.53
6		5	0.05	0.75	2.40	-5.69	-1.69	10.45
7	350	1	0.05	0.7	2.19	-3.97	-1.52	3.33
8		3	0.1	0.8	2.18	-4.58	-1.91	8.99
9		5	0.05	0.8	2.15	-5.80	-1.58	14.72

and Fig. 6 C compare $\overline{T}$ of P over N and R respectively. In each plot, the colors map to the range between the maximum (red) and minimum (blue) value. In addition, in Fig. 6 B and Fig. 6 C, red coloring corresponds with $\overline{T}$ increasing while blue coloring corresponds with $\overline{T}$ decreasing. In white colored cells, there has been no change in $\overline{T}$. Lastly, Tab. II shows the results for the best performing E_r and X_r for each combination of N_b and W_s, highlighted with numbered yellow boxes in Fig. 6.

V. DISCUSSION

As can be observed in Fig. 6 A, $\overline{T}$ in P ranges between 2-3 minutes. The predominant effect in $\overline{T}$ comes from the variation in N_b. In other words, the greater the number of vehicles, the shorter the wait times, because the likelihood of finding an available bicycle in close proximity is higher.

The proposed rebalancing strategy can be assessed by comparing the P and N scenarios (Fig. 6 B). It can be observed that the $\overline{T}$ decreases significantly in almost all parameter configurations, reaching reductions of up to 5.8% in $\overline{T}$, showing that the strategy is effective. Only one parameter combination showed a slight deterioration in service, with an increase of 0.22% in wait time. This small variation is considered a consequence of the stochastic nature of the system, and would be expected to follow the general trend with an increased number of simulations. The improvement is most significant in medium or large N_b. When vehicles rebalance, the batteries discharge at a higher rate and bicycles need to swap their batteries more frequently, consequently decreasing the number of available bicycles. In medium and high N_b scenarios, the system can afford having some vehicles charging and still provide low wait times. However, in scenarios with low N_b the reduced availability has a more significant impact on level of service and, as a consequence, the proposed rebalancing strategy is less beneficial. At the same time, for medium and high N_b, the improvement is greater in scenarios with higher W_s. This is because faster-moving vehicles enable the system to be more responsive to changes in demand.

Comparing the P and R scenarios shows the reduction in $\overline{T}$ that is attributable to self-driving rebalancing in general (even with basic random movement) versus the reduction attributable specifically to our proposed stigmergic behavior. As can be observed in Fig. 6 C, these results show a high dependency on the combinations of parameters. This dependency indicates that, for the stigmergy strategy to outperform the random scenario, E_r and X_r need to be adjusted for each N_b and W_s. A similar behavior can be observed in [50].

Parameter tuning is needed because of the different trade-offs present in complex systems (e.g., exploitation vs. exploration). For instance, a low E_r fosters the formation of pheromone trails that persist over time, guiding the system towards identified demand areas (i.e., exploitation). However, if the rate is too low, it can lead to trail saturation, hindering the system's ability to explore new paths. Similarly, a low X_r is detrimental to the system's ability to exploit identified demand areas, but it helps in exploring new ones (i.e., exploration).

As can be observed in Fig. 6, most N_b and W_s combinations perform best with a low E_r (0.05), indicating that the system benefits from having pheromone trails persist for a longer time. In terms of X_r, instead, most scenarios benefit from a medium-high X_r, which means that the system will be effective in exploiting already found paths, but still keeping some randomness to find new, unexplored solutions. At the same time, these system-level behaviors can also depend on N_b and W_s. For instance, it can be observed how the scenario with highest N_b and W_s is the one that most benefits from higher exploitation ($E_r = 0.8$) since having more vehicles that travel faster, the system is already exploring more solutions, and therefore, randomness is less critical.

Tab. II shows the results for each combination of N_b and W_s with the best performing E_r and X_r. In these results, it can be observed that, once E_r and X_r are tuned, the P scenario reduces $\overline{T}$ in a range of [1.76-5.8]% compared to N and [1.16-2.03]% compared to R. In Tab. II, the rightmost column represents the additional distance traveled by the bicycle fleet in P and R compared to N. It can be observed that the distances increase significantly with increased W_s, particularly for large N_b. These results indicate that, while adjusting the fleet size and wandering speed parameters of the proposed stigmergy-based rebalancing strategy, one should consider that increasing the number of bicycles decreases the wait times, but this might carry economic and environmental costs. Similarly, increasing the wandering speed can improve the wait time only slightly and carries the associated cost of greatly increasing the total traveled distance.

The proposed approach has two main limitations that should be noted. First, the evaporation and exploitation rates must be appropriately tuned to get the desired behavior, which may be scenario-dependent. Second, the total distance traveled can increase significantly, especially for high wandering speeds and large fleet sizes. To address this issue, future work could explore dynamic methods for adjusting the wandering speed based on the level of pheromones detected. For example, vehicles could move slowly during periods of low activity and faster during times of high demand. In addition to addressing these limitations, future work could in-

vestigate the potential of applying similar decentralized bio-inspired processes for other tasks such as battery swapping or task allocation. Furthermore, implementing the developed algorithm on actual autonomous vehicles and validating it with real users in urban environments would be an important step toward practical implementation.

VI. Conclusions

The current trends in urban transportation systems point toward electrification, autonomy, and sharing. However, these solutions are challenging to coordinate in a centralized manner, and decentralized planning with self-driving vehicles in shared micro-mobility systems has rarely been studied. Inspired by work in the field of swarm robotics, this paper presents a fully decentralized approach for a fleet of shared autonomous bicycles to self-organize their own rebalancing. The proposed approach is inspired by natural stigmergy in social insects and has been analyzed in a multi-layer agent-based simulation based on real data for an example urban area. The results indicate that the system is effective in rebalancing the bicycles in a self-organized way, significantly reducing the wait times and improving user experience compared to random rebalancing or the absence of rebalancing. This study shows that, in order to obtain good rebalancing performance using our proposed system, the parameters need to be appropriately tuned. For example, one important trade-off is that increasing the number of vehicles or their speed reduces wait times but undesirably increases the total distance traveled. Overall, the results indicate that self-organized approaches could be suitable to address the planning challenges presented by increasingly complex new mobility systems.

References

[1] E. Cascetta, *Transportation systems analysis: models and applications*. Springer Science & Business Media, 2009, vol. 29.

[2] N. C. Sanchez, L. A. Pastor, and K. Larson, "Autonomous bicycles: A new approach to bicycle-sharing systems," in *2020 IEEE 23rd International Conference on Intelligent Transportation Systems (ITSC)*. IEEE, 2020, pp. 1–6.

[3] S. Liu and J.-L. Gaudiot, "Autonomous vehicles lite self-driving technologies should start small, go slow," *IEEE Spectrum*, vol. 57, no. 3, pp. 36–49, 2020.

[4] M. C.-L. Lin, "Affordable autonomous lightweight personal mobility," Ph.D. dissertation, Massachusetts Institute of Technology, 2021.

[5] N. C. Sanchez, I. Martinez, L. A. Pastor, and K. Larson, "On the simulation of shared autonomous micro-mobility," *Communications in Transportation Research*, vol. 2, p. 100065, 2022.

[6] N. Coretti Sanchez, I. Martinez, L. A. Pastor, and K. Larson, "On the performance of shared autonomous bicycles: A simulation study," *Communications in Transportation Research*, vol. 2, p. 100066, 2022.

[7] D. Kondor, X. Zhang, M. Meghjani, P. Santi, J. Zhao, and C. Ratti, "Estimating the potential for shared autonomous scooters," *IEEE Transactions on Intelligent Transportation Systems*, vol. 23, no. 5, pp. 4651–4662, 2021.

[8] W. Schwarting, J. Alonso-Mora, and D. Rus, "Planning and decision-making for autonomous vehicles," *Annual Review of Control, Robotics, and Autonomous Systems*, vol. 1, no. 1, pp. 187–210, 2018.

[9] P. M. Boesch, F. Ciari, and K. W. Axhausen, "Autonomous vehicle fleet sizes required to serve different levels of demand," *Transportation Research Record*, vol. 2542, no. 1, pp. 111–119, 2016.

[10] O. Dlugosch, T. Brandt, and D. Neumann, "Combining analytics and simulation methods to assess the impact of shared, autonomous electric vehicles on sustainable urban mobility," *Information & Management*, p. 103285, 2020.

[11] K. Dorer and M. Calisti, "An adaptive solution to dynamic transport optimization," in *Proceedings of the fourth international joint conference on Autonomous agents and multiagent systems*, 2005, pp. 45–51.

[12] L. Marrocco, E. C. Ferrer, A. Bucchiarone, A. Grignard, L. Alonso, K. Larson, and A. Pentland, "Basic: Towards a blockchained agent-based simulator for cities," in *International Workshop on Massively Multiagent Systems*. Springer, 2018, pp. 144–162.

[13] L. Duan, Y. Wei, J. Zhang, and Y. Xia, "Centralized and decentralized autonomous dispatching strategy for dynamic autonomous taxi operation in hybrid request mode," *Transportation Research Part C: Emerging Technologies*, vol. 111, pp. 397–420, 2020.

[14] A. Bucchiarone, "Collective adaptation through multi-agents ensembles: The case of smart urban mobility," *ACM Transactions on Autonomous and Adaptive Systems (TAAS)*, vol. 14, no. 2, pp. 1–28, 2019.

[15] A. Kapitonov, S. Lonshakov, I. Berman, E. C. Ferrer, F. P. Bonsignorio, V. Bulatov, and A. Svistov, "Robotic services for new paradigm smart cities based on decentralized technologies," *Ledger*, 2019.

[16] H. Si, J. gang Shi, G. Wu, J. Chen, and X. Zhao, "Mapping the bike sharing research published from 2010 to 2018: A scientometric review," *Journal of Cleaner Production*, vol. 213, pp. 415 – 427, 2019.

[17] A. Kaltenbrunner, R. Meza, J. Grivolla, J. Codina, and R. Banchs, "Urban cycles and mobility patterns: Exploring and predicting trends in a bicycle-based public transport system," *Pervasive and Mobile Computing*, vol. 6, no. 4, pp. 455 – 466, 2010, human Behavior in Ubiquitous Environments: Modeling of Human Mobility Patterns.

[18] J.-H. Lin and T.-C. Chou, "A geo-aware and VRP-based public bicycle redistribution system," *International Journal of Vehicular Technology*, vol. 2012, 2012.

[19] S. He and K. G. Shin, "Dynamic flow distribution prediction for urban dockless e-scooter sharing reconfiguration," in *Proceedings of The Web Conference 2020*, 2020, pp. 133–143.

[20] H. Luo, Z. Kou, F. Zhao, and H. Cai, "Comparative life cycle assessment of station-based and dock-less bike sharing systems," *Resources, Conservation and Recycling*, vol. 146, pp. 180–189, 2019.

[21] J. Büttner, H. Mlasowsky, T. Birkholz, *et al.*, "Optimising bike sharing in european cities-a handbook. obis project," 2011.

[22] D. Chemla, F. Meunier, and R. W. Calvo, "Bike sharing systems: Solving the static rebalancing problem," *Discrete Optimization*, vol. 10, no. 2, pp. 120–146, 2013.

[23] M. Dell'Amico, E. Hadjicostantinou, M. Iori, and S. Novellani, "The bike sharing rebalancing problem: Mathematical formulations and benchmark instances," *Omega*, vol. 45, pp. 7–19, 2014.

[24] M. Dell, M. Iori, S. Novellani, T. Stützle, *et al.*, "A destroy and repair algorithm for the bike sharing rebalancing problem," *Computers & Operations Research*, vol. 71, pp. 149–162, 2016.

[25] J. Schuijbroek, R. C. Hampshire, and W.-J. Van Hoeve, "Inventory rebalancing and vehicle routing in bike sharing systems," *European Journal of Operational Research*, vol. 257, no. 3, pp. 992–1004, 2017.

[26] F. Chiariotti, C. Pielli, A. Zanella, and M. Zorzi, "A dynamic approach to rebalancing bike-sharing systems," *Sensors*, vol. 18, no. 2, p. 512, 2018.

[27] A. Pal and Y. Zhang, "Free-floating bike sharing: Solving real-life large-scale static rebalancing problems," *Transportation Research Part C: Emerging Technologies*, vol. 80, pp. 92–116, 2017.

[28] M. Du, L. Cheng, X. Li, and F. Tang, "Static rebalancing optimization with considering the collection of malfunctioning bikes in free-floating bike sharing system," *Transportation Research Part E: Logistics and Transportation Review*, vol. 141, p. 102012, 2020.

[29] C. Lu, L. Gao, and Y. Huang, "Exploring travel patterns and static rebalancing strategies for dockless bike-sharing systems from multi-source data: a framework and case study," *Transportation Letters*, pp. 1–14, 2022.

[30] D. Barabonkov, S. D'Alonzo, J. Pierre, D. Kondor, X. Zhang, and M. A. Tien, "Simulating and evaluating rebalancing strategies for dockless bike-sharing systems," *arXiv preprint arXiv:2004.11565*, 2020.

[31] Z. Haider, A. Nikolaev, J. E. Kang, and C. Kwon, "Inventory rebalancing through pricing in public bike sharing systems," *European Journal of Operational Research*, vol. 270, no. 1, pp. 103–117, 2018.

[32] F. Chiariotti, C. Pielli, A. Zanella, and M. Zorzi, "A bike-sharing optimization framework combining dynamic rebalancing and user incentives," *ACM Transactions on Autonomous and Adaptive Systems (TAAS)*, vol. 14, no. 3, pp. 1–30, 2020.

[33] H. Jin, S. Liu, K. C. So, and K. Wang, "Dynamic incentive schemes for managing dockless bike-sharing systems," *Transportation Research Part C: Emerging Technologies*, vol. 136, p. 103527, 2022.

[34] J. Alonso-Mora, S. Samaranayake, A. Wallar, E. Frazzoli, and D. Rus, "On-demand high-capacity ride-sharing via dynamic trip-vehicle assignment," *Proceedings of the National Academy of Sciences*, vol. 114, no. 3, pp. 462–467, 2017.

[35] R. Zhang and M. Pavone, "Control of robotic mobility-on-demand systems: a queueing-theoretical perspective," *The International Journal of Robotics Research*, vol. 35, no. 1-3, pp. 186–203, 2016.

[36] D. J. Fagnant and K. M. Kockelman, "The travel and environmental implications of shared autonomous vehicles, using agent-based model scenarios," *Transportation Research Part C: Emerging Technologies*, vol. 40, pp. 1–13, 2014.

[37] T. Babicheva, W. Burghout, I. Andreasson, and N. Faul, "The matching problem of empty vehicle redistribution in autonomous taxi systems," *Procedia computer science*, vol. 130, pp. 119–125, 2018.

[38] F. Rossi, R. Zhang, Y. Hindy, and M. Pavone, "Routing autonomous vehicles in congested transportation networks: Structural properties and coordination algorithms," *Autonomous Robots*, vol. 42, no. 7, pp. 1427–1442, 2018.

[39] F. Dandl, M. Hyland, K. Bogenberger, and H. S. Mahmassani, "Evaluating the impact of spatio-temporal demand forecast aggregation on the operational performance of shared autonomous mobility fleets," *Transportation*, vol. 46, no. 6, pp. 1975–1996, 2019.

[40] M. Guériau and I. Dusparic, "Samod: Shared autonomous mobility-on-demand using decentralized reinforcement learning," in *2018 21st International Conference on Intelligent Transportation Systems (ITSC)*. IEEE, 2018, pp. 1558–1563.

[41] E. C. Ferrer, "If blockchain is the solution, robot security is the problem," *Frontiers in Blockchain*, vol. 6, 2023. [Online]. Available: https://www.frontiersin.org/articles/10.3389/fbloc.2023.1181820

[42] J. Harding, G. Powell, R. Yoon, J. Fikentscher, C. Doyle, D. Sade, M. Lukuc, J. Simons, J. Wang, *et al.*, "Vehicle-to-vehicle communications: readiness of v2v technology for application." United States. National Highway Traffic Safety Administration, Tech. Rep., 2014.

[43] E. C. Ferrer, T. Hardjono, A. Pentland, and M. Dorigo, "Secure and secret cooperation in robot swarms," *Science Robotics*, vol. 6, no. 56, p. eabf1538, 2021. [Online]. Available: https://www.science.org/doi/abs/10.1126/scirobotics.abf1538

[44] E. Bonabeau, D. d. R. D. F. Marco, M. Dorigo, G. Théraulaz, G. Theraulaz, *et al.*, *Swarm intelligence: from natural to artificial systems*. Oxford university press, 1999, no. 1.

[45] E. Sahin, "Swarm robotics: From sources of inspiration to domains of application," in *Swarm Robotics*, 2004.

[46] G. Beni, "From swarm intelligence to swarm robotics," in *International Workshop on Swarm Robotics*. Springer, 2004, pp. 1–9.

[47] M. Rubenstein, A. Cornejo, and R. Nagpal, "Programmable self-assembly in a thousand-robot swarm," *Science*, vol. 345, no. 6198, pp. 795–799, 2014.

[48] M. Brambilla, E. Ferrante, M. Birattari, and M. Dorigo, "Swarm robotics: a review from the swarm engineering perspective," *Swarm Intelligence*, vol. 7, no. 1, pp. 1–41, 2013.

[49] P. A. López Matencio Pérez, J. Vales Alonso, E. Costa Montenegro, *et al.*, "Ant: Agent stigmergy-based iot-network for enhanced tourist mobility," 2017.

[50] A. L. Alfeo, M. G. C. Cimino, S. Egidi, B. Lepri, A. Pentland, and G. Vaglini, "Stigmergy-based modeling to discover urban activity patterns from positioning data," in *International Conference on Social Computing, Behavioral-Cultural Modeling and Prediction and Behavior Representation in Modeling and Simulation*. Springer, 2017, pp. 292–301.

[51] A. L. Alfeo, E. C. Ferrer, Y. L. Carrillo, A. Grignard, L. A. Pastor, D. T. Sleeper, M. G. Cimino, B. Lepri, G. Vaglini, K. Larson, *et al.*, "Urban swarms: A new approach for autonomous waste management," in *2019 International Conference on Robotics and Automation (ICRA)*. IEEE, 2019, pp. 4233–4240.

[52] Q. Lu, M. E. Moses, and J. P. Hecker, "A scalable and adaptable multiple-place foraging algorithm for ant-inspired robot swarms," *arXiv preprint arXiv:1612.00480*, 2016.

[53] M. Dorigo, E. Bonabeau, and G. Theraulaz, "Ant algorithms and stigmergy," *Future Generation Computer Systems*, vol. 16, no. 8, pp. 851–871, 2000. [Online]. Available: https://www.sciencedirect.com/science/article/pii/S0167739X0000042X

[54] J. Li, E. Rombaut, and L. Vanhaverbeke, "A systematic review of agent-based models for autonomous vehicles in urban mobility and logistics: Possibilities for integrated simulation models," *Computers, Environment and Urban Systems*, vol. 89, p. 101686, 2021.

[55] A. Grignard, P. Taillandier, B. Gaudou, D. A. Vo, N. Q. Huynh, and A. Drogoul, "Gama 1.6: Advancing the art of complex agent-based modeling and simulation," in *International conference on principles and practice of multi-agent systems*. Springer, 2013, pp. 117–131.

[56] P. Taillandier, B. Gaudou, A. Grignard, Q.-N. Huynh, N. Marilleau, P. Caillou, D. Philippon, and A. Drogoul, "Building, composing and experimenting complex spatial models with the gama platform," *GeoInformatica*, vol. 23, no. 2, pp. 299–322, 2019.

[57] B. Gaudou, N. Q. Huynh, D. Philippon, A. Brugière, K. Chapuis, P. Taillandier, P. Larmande, and A. Drogoul, "Comokit: A modeling kit to understand, analyze, and compare the impacts of mitigation policies against the covid-19 epidemic at the scale of a city," *Frontiers in public health*, p. 587, 2020.

[58] L. Alonso, Y. R. Zhang, A. Grignard, A. Noyman, Y. Sakai, M. ElKatsha, R. Doorley, and K. Larson, "Cityscope: a data-driven interactive simulation tool for urban design. use case volpe," in *International conference on complex systems*. Springer, 2018, pp. 253–261.

[59] A. Grignard, L. Alonso, P. Taillandier, B. Gaudou, T. Nguyen-Huu, W. Gruel, and K. Larson, "The impact of new mobility modes on a city: A generic approach using abm," in *International Conference on Complex Systems*. Springer, 2018, pp. 272–280.

[60] Bluebikes, "Bluebikes system data," 2020. [Online]. Available: https://www.bluebikes.com/system-data

[61] OpenStreetMap, "Planet dump retrieved from https://planet.osm.org ," 2017.

[62] K. Larson, N. Coretti Sanchez, and M. Lin, "Methods and apparatus for reconfigurable autonomous vehicle," US Patent Application US2021012244, Oct, 2020.

[63] R. C. Browning, E. A. Baker, J. A. Herron, and R. Kram, "Effects of obesity and sex on the energetic cost and preferred speed of walking," *Journal of Applied Physiology*, vol. 100, no. 2, pp. 390–398, 2006.

[64] P. Jensen, J.-B. Rouquier, N. Ovtracht, and C. Robardet, "Characterizing the speed and paths of shared bicycle use in lyon," *Transportation Research Part D: Transport and Environment*, vol. 15, no. 8, pp. 522–524, 2010.

[65] N. Sanchez, L. A. Pastor, and K. Larson, "Can autonomy make bicycle-sharing systems more sustainable? an environmental impact analysis," *Transportation research part D: transport and environment*, vol. 113, p. 103489, 2022.

[66] F.-H. Huang, "Understanding user acceptance of battery swapping service of sustainable transport: An empirical study of a battery swap station for electric scooters, taiwan," *International Journal of Sustainable Transportation*, vol. 14, no. 4, pp. 294–307, 2020.